

AE



LABORATORI NAZIONALI DI FRASCATI

SIS – Pubblicazioni

LNF-94/050 (P)
23 September 1994

LEE-YANG Zeros and the Chiral Phase Transition in Compact Lattice QED

V. Azcoiti

Departamento de Fisica Teorica, Facultad de Ciencias, Universidad de Zaragoza,
50009 Zaragoza, SPAIN

I. M. Barbour

Dept. of Physics and Astronomy, University of Glasgow, Glasgow G12 8QQ, U.K.

R. Burioni

INFN Sezione di Roma I, Dipartimento di Fisica, I Universita' di Roma "La Sapienza",
I-00185 Rome, ITALY

G. Di Carlo, A. F. Grillo

INFN – Laboratori Nazionali di Frascati, POB 13, I-00044 Frascati, ITALY

and G. Salina

INFN Sezione di Roma II, Dipartimento di Fisica
II Universita' di Roma "Tor Vergata", I-00133 Rome, ITALY

su 9507



SCAN-9502064

CERN LIBRARIES, GENEVA

Abstract

In this paper we present a detailed study of the phase structure in the β - m plane for Compact Lattice QED. We analyse the scaling properties of the distribution of the partition function zeros in the complex fermion mass plane on 4^4 , 6^4 , 8^4 and 10^4 lattices. The partition function is numerically evaluated by using two independent methods, based respectively on a standard HMC (Hybrid Monte Carlo) and on an alternative approach derived from the MFA (Microcanonical Fermionic Average). The finite size scaling behaviour gives strong indications for a first order phase transition at any value of the fermion mass. The reliability of the result follows from the remarkable agreement between the two independent methods.

PACS.: 11.15.Ex; 11.30.Rd; 64.60.Fr

(Submitted to Phys. Rev. D)

1 Introduction

The lattice approach to quantum field theories is a mathematically well defined way to extract results in the non perturbative regime; being a regularization scheme, the lattice formulation has to be connected with the continuum limit, which is supposed to describe the real theory, through a renormalization procedure. The equivalence can be meaningful only when the effects of the discretisation of space-time become negligible, i.e. when the system is scale invariant. This is known to happen in the case of a second order phase transition. The knowledge of the phase diagram of the corresponding statistical mechanical system is therefore crucial in order to establish the existence of the theory in the continuum and to make predictions about its physical properties.

The critical behaviour of a statistical system can be investigated using several different approaches; one of the most direct is the study of the Lee-Yang zeros [1], i.e. the zeros of the analytical continuation of the partition function for complex values of the critical parameter. The thermodynamical functions can be reconstructed from Lee-Yang zeros and the critical properties of the theory in the continuum can be inferred from the dependence of the thermodynamical functions on the volume.

The Lee-Yang method has been used to investigate the critical properties of several statistical models, both analytically and numerically. Recently the numerical approach has been extended to lattice gauge theories with and without dynamical fermions [2], [3]: several results have been obtained in small lattices for QED and QCD in 4 dimensions [4], [5], [6]. In particular great interest has been devoted to the Abelian model; indeed the existence of a continuum limit for this model is very interesting because it would provide an example of a 4-dimensional non asymptotically free quantum field theory. From this point of view the two possible formulations for the Abelian model on a lattice seem to present very different features.

For Non Compact Lattice QED there are strong evidences of the system undergoing a continuous transition while it has not been clarified yet if the theory is interacting in the continuum limit [7].

The situation for the Compact formulation is different: in the quenched limit it has been almost established [8] that the model presents a first order phase transition at a finite value of the coupling constant. For the theory to exist in the continuum, the introduction of light fermions has to modify the character of the transition, making it second order. The problem has not been clarified yet, even if there are indications of a strengthening [9] of the quenched phase transition after the introduction of light fermions. On the other hand, previous calculations have not shown the expected scaling behaviour for Lee-Yang zeros [10]. A deeper study of the situation is therefore of great interest.

In this paper we present a comprehensive analysis of Lee-Yang zeros for Compact Lattice QED in order to give a definitive answer to the problem.

To this purpose we use two independent methods for the reconstruction of the partition function and we analyse data for 4 different volumes, from 4^4 to 10^4 in order to have an accurate estimation of the scaling exponents. Moreover, one of the two approaches (namely MFA [11]), does not require a separate fermionic simulation for each β , thus allowing to extend the analysis to the whole relevant β range.

The main result of our analysis is a strong evidence of the persistence of a discontinuous transition down to $m = 0$.

The paper is organized as follows: in section 2 we review the theoretical framework for the computation of the partition function as a polynomial in the mass; in section 3 we describe the numerical methods used for the generation of the configurations and for the root finder; in section 4 we compare the results obtained at 4^4 and 6^4 with both methods; in section 5 we study the phase diagram of the model and the scaling exponents from the MFA data. Finally, section 6 contains our conclusions.

2 The model and the Lee-Yang zeros

The discretization on a 4-dimensional lattice of Compact QED leads to the following action:

$$S = \frac{1}{2} \sum_{x,\mu} \eta_\mu(x) \bar{\chi}(x) \{ U_\mu(x) \chi(x + \mu) - U_\mu^*(x - \mu) \chi(x - \mu) \} + m \sum_x \bar{\chi}(x) \chi(x) + \beta \sum_{x,\mu < \nu} (1 - \cos(U_{\mu\nu}(x))) = S_F + \beta S_G \quad (1)$$

where

$$U_{\mu\nu}(x) = U_\mu(x) U_\nu(x + \hat{\mu}) U_\mu^*(x + \hat{\nu}) U_\nu^*(x) \quad (2)$$

and $\chi(x)$ are the Kogut-Susskind fermion fields, describing 4 degenerate flavours, and $U_\mu(x)$ represents the compact link variable. The introduction of the Kogut-Susskind formulation for the fermion fields is here justified by the fact that we are interested in the chiral properties of the model. The lattice theory described by (1) can be regarded as a statistical model, whose partition function depends on two external parameters, namely the inverse coupling constant $\beta = \frac{1}{e^2}$ and the bare fermion mass m :

$$Z(\beta, m) = \int [d\chi][d\bar{\chi}][dU_\mu(x)] e^{-S} \quad (3)$$

The integration over the Grassmann variables can be explicitly taken and gives

$$Z(\beta, m) = \int [dU_\mu(x)] \det M[m, U_\mu(x)] e^{-\beta S_G} \quad (4)$$

where M is the fermionic matrix:

$$M(n, m) = m \delta_{n,m} + \sum_\mu \frac{1}{2} \delta_{n,x} \eta_\mu(x) (\delta_{m,x+\mu} U_\mu(x) - \delta_{m,x-\mu} U_\mu^*(x - \mu)). \quad (5)$$

The fermionic matrix M can thus be decomposed as:

$$M = m \cdot I + \Delta \quad (6)$$

where Δ is an antihermitian matrix. The characteristic form of M implies that for every gauge field configuration the determinant can be written as a polynomial in the mass m [5]:

$$\det M = \sum_n C_n [U_\mu] m^n \quad (7)$$

At fixed β , the partition function is then, formally, proportional to the expectation value of the fermionic determinant taken over pure gauge fields configurations and can be written as a polynomial in the fermion mass:

$$Z_\beta(m) = \int [dU_\mu(x)] e^{-\beta S_G} \sum_n C_n [U_\mu] m^n = \sum_n C_n(\beta) m^n \quad (8)$$

In this formulation, the polynomial (7) has degree equal to the volume of the system. Its even coefficients are positive and the odd ones are identically zero.

Equation (8) is the starting point for the Lee-Yang approach to the study of the chiral phase transition, which requires the determination of the zeros of the partition function in the complex mass plane.

Here one expects the standard scenario for the zeros of the partition function of a general statistical system. The complex zeros are expected to arrange themselves in regular structures, for example lines, which separate regions of the parameter space where the partition function has different properties [12].

The complete set is needed in order to reconstruct the thermodynamical functions of the model but the critical properties of the system are only determined by the zeros lying closest to the real axis [1], which are directly related to the singular part of the partition function. Indeed the system presents a discontinuity in some derivatives of the free energy when one of these regular patterns cuts the positive real axis in the thermodynamical limit. In particular the critical points of the model coincide with the zeros lying on the real axis.

At finite volume the partition function (8) has a finite number of complex zeros lying outside a region surrounding the real axis: this guarantees the analyticity of the partition functions (8). At increasing finite volume the sequence of the real parts of the zero lying nearest to the real axis (critical zeros) converges to the critical point. Several conjectures have been suggested relating the order of the phase transition with the geometrical distribution of the zeros [3] and with the scaling behaviour of the imaginary parts of the critical zeros with increasing volumes [4], although no rigorous proof has been given yet.

Compact QED is known to undergo a phase transition at a finite value of the coupling constant for every value of the mass [13], [9]. In particular the critical value of β is always non zero and it decreases with decreasing mass (Fig.1a). At fixed beta the zeros are distributed in three different types of patterns [14]: for $\beta < \beta_c(m=0)$ all the zeros are pure imaginary and they cut the real axis at $m=0$ (Fig.1b); for $\beta > \beta_c(m=\infty)$ the situation is similar but the zeros do not cut the real axis anymore (Fig.1c); in the intermediate region the zeros are pure imaginary down to a given value of the imaginary part and then they migrate into the complex plane forming a curve that cuts the real axis at $m = m_c > 0$ (Fig.1d).

In the $\beta - m$ plane the critical points form a line that join the quenched critical point ($m \rightarrow \infty$), where the transition is known to be first order [8], to the chiral

limit ($m = 0$) where a real physical theory should be defined. The existence of the theory in the continuum limit would then require a change in the order of the phase transition along the critical line.

There are several interesting quantities related to the order of the transition [4]. For a continuous phase transition, from general finite size scaling arguments, the position of the critical zero in the complex plane is ruled by the scaling law:

$$z_c(L) - z_c(\infty) = AL^{-\frac{1}{\nu}}, \quad (9)$$

where A is a complex number. This means that the real and the imaginary part of the zero scale independently with the same exponent. Namely:

$$\mathcal{R}e z_c(L) - z_c(\infty) \sim L^{-\frac{1}{\nu}} \quad (10)$$

and

$$\mathcal{I}m z_c(L) \sim L^{-\frac{1}{\nu}}. \quad (11)$$

The scaling law (11) can be extended to the case of a first order phase transition, where the shift is determined only by the actual size of the system, due to the fact that there is no divergent correlation length. In this case, for a 4-dimensional model we expect $\frac{1}{\nu} = 4$. On the other hand the exponent of the real part of the critical zero is not supposed to present an universal behaviour [4].

Another interesting relation for a second order phase transition is the scaling law for the linear density of the zeros near to the real axis as a function of the linear size of the lattice:

$$\rho(L) \sim L^\gamma. \quad (12)$$

Again this scaling law can be expected to hold also for a first order transition with $\gamma = 4$.

3 The numerical approaches

The lattice approach to the computation of the mass dependence of the partition function amounts to the determination of the coefficients in (8). In general, the functional integration over the gauge fields in (4) can be performed numerically using a Monte Carlo scheme for the generation of statistically independent gauge configuration from the correct probability distribution.

One of the main problems arising in the measurement of the expectation value of the fermion determinant is that there may be no overlap between the probability distribution of the pure gauge fields with the effective support of the operator (7) and this spoils the convergence of the averaging procedure. The problem can be faced using different approaches related to different numerical algorithm. Here we will discuss in details two of them: the Hybrid Monte Carlo method (HMC) [15] and the Microcanonical Fermionic Average (MFA) [11].

In the HMC approach the problem is solved shifting the probability distribution of the gauge fields by introducing an updating mass m_0 [5]. This procedure corresponds to measure a new operator that can be analytically related to the old

fermionic determinant. The support of new operator overlaps with the shifted probability distribution, at least for m belonging to a neighborhood of m_0 .

We briefly recall the main steps leading to this modification of the operator: at fixed β , using the irrelevance of overall multiplicative factors in the partition function, we can write:

$$\begin{aligned} Z_\beta(m) \sim \frac{Z_\beta(m)}{Z_\beta(m_0)} &= \frac{\int [dU_\mu] \det M(m) e^{-\beta S_G}}{\int [dU_\mu] \det M(m_0) e^{-\beta S_G}} \\ &= \frac{\int [dU_\mu] \frac{\det M(m)}{\det M(m_0)} \det M(m_0) e^{-\beta S_G}}{\int [dU_\mu] \det M(m_0) e^{-\beta S_G}} \\ &= \left\langle \frac{\det M(m)}{\det M(m_0)} \right\rangle_{P(m_0, \beta)} \end{aligned} \quad (13)$$

Therefore the partition function can be expressed as the vacuum expectation value of the determinant ratio $\det M(m)/\det M(m_0)$, averaged over configurations generated with probability weight

$$P[U_\mu, m_0, \beta] = \frac{\det M[m_0, U] e^{-\beta S_G[U]}}{\int [dU'] \det M[m_0, U'] e^{-\beta S_G[U']}}. \quad (14)$$

Using the fact that $\det M(m)$ is a polynomial in the mass we can write

$$\frac{\det M(m)}{\det M(m_0)} = \sum_{n=0}^{V/2} C_n(\beta) \frac{m^{2n}}{\det M(m_0)}. \quad (15)$$

This procedure obviously does not change the zeros of the partition function.

At every β value the configurations for the gauge fields are generated, following the new distribution (14), with a standard HMC code. For a single configuration a modified Lanczos algorithm [16] gives the eigenvalues λ_i of the massless fermionic matrix Δ (6), which are pure imaginary. The coefficients are then computed from the eigenvalues and then averaged over the configurations: they are the fundamental quantities for the determination of the zeros of the polynomial.

The coefficients of the partition function can be computed in a completely independent way in the MFA framework [11].

The basic idea in MFA is the exploitation of the physical equivalence between the canonical and the microcanonical formalism, in our case the introduction of an explicit dependence on the energy in the computation of the partition function. Indeed (4) can be written as follows:

$$Z(\beta, m) = \int dE n(E) e^{-6V\beta E} \overline{\det M(E, m)} \quad (16)$$

where

$$n(E) = \int [dU_\mu] \delta(6VE - S_G[U_\mu]) \quad (17)$$

is the density of state at fixed energy E and

$$\overline{\det M(E, m)} = \frac{\int [dU_\mu] \delta(6VE - S_G[U_\mu]) \det M[m, U_\mu]}{n(E)} \quad (18)$$

is the fermionic determinant averaged over field configurations of fixed energy E . Note that (18) does not depend on β . As stated before, the fermionic determinant for a single configuration is a polynomial in the mass:

$$\det M[U_\mu, m] = \sum_n C_n[U_\mu] m^n \quad (19)$$

and therefore also (18) can be rewritten as a polynomial in the mass:

$$\overline{\det} M(E, m) = \sum_n C_n(E) m^n \quad (20)$$

with coefficient depending on the energy:

$$C_n(E) = \frac{\int [dU_\mu] \delta(6VE - S_G[U_\mu]) C_n[U_\mu]}{n(E)}. \quad (21)$$

Substituting (20) in the partition function (16) we obtain the key relation between the coefficients, as defined in the previous formalism, and the microcanonical quantities:

$$C_n(\beta) = \int dE n(E) e^{-6V\beta E} C_n(E). \quad (22)$$

The explicit computation of the coefficients then requires the knowledge of both the coefficients $C_n(E)$ and the density of states $n(E)$: here the latter quantity is obtained numerically.

This is done evaluating P_{β_0} , the pure gauge probability distribution of the plaquette S_G at some fixed β_0 (i.e. the histogram of the plaquette) [9]. In a finite range of energies, depending on the selected value of β_0 , P_{β_0} can be related to $n(E)$:

$$n(E) \sim P_{\beta_0}(E) e^{6V\beta_0 E} \quad (23)$$

In general, for the evaluation of the integral in (22) $n(E)$ must be evaluated in a wider range of energies, therefore one can repeat this calculation, using a series of values of β_0 and then reconstructing the density of state by normalizing the overlapping distributions at adjacent values of β_0 . The number of different values of β_0 , near a phase transition, increases with the volume of the system, varying, in our lattices, from 5 (in the 4^4) to 20 (in the 10^4).

For the calculation of $C_n(E)$ we proceed as follows: first we chose a set of values of energy, in the range selected to cover the support of the weight function in (22), for the values of β we are interested in. Then for every value of E in the set we generate gauge fields configuration using a microcanonical code (in this case standard overrelaxation [17]); the generation of gauge fields at fixed energy is not the costly part of the whole procedure, so we can well decorrelate the configurations used for measuring the fermionic operator. Again a modified Lanczos algorithm is used in order to obtain the complete set of eigenvalues of the massless fermion matrix Δ , and the coefficients $C_n(E)$ are reconstructed recursively and then averaged over decorrelated configurations. The scheme is essentially the same used in a typical MFA calculation [11], [9].

At the end we have the coefficients $C_n(E)$ evaluated at discrete energy values: a polynomial interpolation allows the reconstruction at arbitrary values of the energy

E , in order to perform the numerical integration in (22) and obtain the coefficients $C_n(\beta)$, that can be regarded, as in the HMC approach, the final product of this part of the numerical procedure for the determination of the Lee Yang zeros. Note that β enters only at this final point, therefore it is possible to determine the coefficients at every β value in an interval defined by the range in energy in which the microcanonical quantities are known, without repeating the costly part of the computation, i.e. the determination of the eigenvalues of the fermionic determinant. Therefore the MFA approach is particularly well suited for a global study of a critical line, like the one existing in Compact Lattice QED.

In this approach the problem of the mismatch between the pure gauge probability distribution and the effective support of the fermionic determinant does not arise.

In fact for an accurate evaluation of the integral (22) one has only to guarantee that the coefficients $C_n(E)$ are computed on the relevant energy values; then the knowledge of the density of states $n(E)$ allows an *a posteriori* reconstruction of the weight function in the integrand. In addition, the microcanonical part of the procedure, i.e. the determination of $C_n(E)$, is completely independent on the subsequent operations, so that one can add some points in energy (if it turns be necessary for the evaluation of the integral in (22)) without having to repeat the complete microcanonical calculation. All these features allows a complete control on the various step in the procedures without any external parameter to be tuned.

As stated before the coefficients $C_n(\beta)$ are the final product of the generation part of our procedure; independently from the scheme used for their calculation, they are the input to the final part, i.e. the determination of the roots of the polynomial (8).

Let us briefly recall the main features of the polynomial: in a volume V , the partition function is a polynomial of order $N = V$ in m and the typical range of the coefficients is of order $e^{V/2}$. With this kind of data the main problem is the efficiency of standard root finders in the determination of the zeros. Here we will use an alternative method [14] developed in order to analyse the partition function. This algorithm is based on well known properties of analytic functions on the complex plane that, in particular, allows the determination of the number of zeros for a given function inside a region of the complex plane, provided the function has no singularities inside this region. In particular, choosing a region R in the complex plane where the function $F(z)$ is differentiable, the number of zeros and poles of $F(z)$ in R is given by:

$$\frac{1}{2i\pi} \oint_L dz \frac{F'(z)}{F(z)} = N - P \quad (24)$$

where the integral is performed on the boundary L of R , N is the number of zeros of the function $F(z)$ in the region R , P is the number of poles, each with its multiplicity. Relation (24) is valid if $F(z)$ has no poles or zeros on L .

In our case, after determining the number of zeros of the partition function in a given region R , we obtain the exact position of the complex zeros by using a minimization procedure on the partition function. A verification is made by calculating the integral on a small circle around the minimum itself and a standard

method (for example Laguerre) refines the numerical value of the zero and increases the precision [14].

This procedure does not present typical problems caused by deflation and slow convergence. Some problems still arise from systematic and statistical errors in the coefficients. However, these errors mainly affect the general distribution of the zeros and do not change the position of the roots lying nearest to the real axis [14].

4 Lee-Yang zeros from HMC and MFA

We now present the results from numerical simulations obtained using the two different methods presented in section (3). In Table 1 we summarize the parameters of the simulations for HMC method and in Table 2 we give the corresponding description for the MFA runs. Note that different boundary conditions for the fermion fields have been used in the two approaches, namely periodic for MFA and antiperiodic for HMC. However some simulations using antiperiodic (periodic) boundary condition were performed in MFA (HMC) to check the influence of boundary conditions on the results.

For every V and β value the coefficients of the partition function have been computed and used to obtain the corresponding zeros in the complex mass plane.

In Fig.2 we present the critical zeros on 4^4 lattice at $\beta = 0.85$ and $\beta = 0.865$ obtained from HMC and MFA. It is evident that the two approaches give consistent results. The absence of significant effects of the boundary conditions on the critical zeros at this volume had been previously checked on HMC [5]. In Fig.3 we show the zeros obtained on 6^4 lattice at $\beta = 0.885$. Here periodic and antiperiodic zeros are presented for MFA while only antiperiodic zeros are shown for HMC. A clear consistency of the whole picture is evident. Antiperiodic zeros obtained from the two methods coincide; a small shift is present between periodic and antiperiodic zeros but this is of the same order of the statistical errors (not present in the figure).

A well defined procedure to obtain statistical errors on Lee-Yang zeros has not been developed and this problem is not discussed in the literature. Here we opted for the following procedure: a standard jackknife method is used to produce n averaged partition functions and n estimations of a given zero. The largest error on the critical zeros is of order 10% on both imaginary and real part. The procedure has been applied to different volumes and the estimate of the error is almost stable.

In Fig.4 we show the phase diagram in the $\beta - m$ plane obtained from 4^4 and 6^4 lattices with MFA and HMC. The estimation of the critical mass is here the real part of the zero lying nearest to the real axis. The consistency of the two approaches at different β values is remarkable, making unnecessary further checks. Note that the critical line is shifted to the right in the $\beta - m$ plane with increasing volume. This strong dependence of the critical β (at fixed mass) on the volume had already been shown in the infinite mass limit [8].

This comparative analysis evidences the complete consistency of the two approaches in the description of the critical properties of the theory. We again emphasize that this agreement on the physical quantities is very remarkable because the two methods use completely different procedures to evaluate the partition function.

From the technical point of view MFA and HMC show different features. In Table 3 we summarize the computer time required to generate the coefficients at different volumes. Due to the use of Lanczos algorithm for the diagonalization of the fermionic matrix both methods have a cost at least of order V^2 . However the influence of the parameters and the decorrelation between subsequent measurements are different. In particular the HMC method requires the introduction and the tuning of an additional parameter, the updating mass m_0 . The tuning becomes more important with increasing volumes, especially in the case of a strong first order phase transition. In Fig.5 we show the critical zeros at $\beta = 0.885$ obtained on 6^4 lattice with three different values of m_0 and the same statistics. By a direct comparison with the MFA zeros shown in Fig.3 it is evident that only for m_0 close to m_c it is possible to obtain the correct zero pattern. In particular the estimate for the critical mass is almost correct but there is a significant shift in the imaginary part. The reliable interval for the tuning of m_0 becomes smaller with increasing volume: on a 4^4 lattice the effects of the change in m_0 are negligible [18].

The estimation for the critical zero on a 8^4 lattice at $\beta = 0.885$ is influenced by this effect. Indeed the critical mass is found to be in agreement with the MFA results but the imaginary part is strongly altered [18].

Because of these problems a direct comparison of the computer cost of the two approaches is not easy. An estimation of the effective computer time for a typical run is given in Table 3.

5 Scaling exponents and the order of the transition

We will now present a detailed analysis of the scaling behavior for the Lee-Yang zeros at 4 different volumes, namely 4^4 , 6^4 , 8^4 and 10^4 . In view of the coincidence of the relevant results of the two approaches, and of the possibility in the MFA approach to move in the theory parameter space at relatively small computer cost, the analysis is carried out using only the MFA data in a wide β range.

In Fig.6 we show the phase diagrams in the $\beta - m$ plane obtained at 4 different volumes. It is evident that the critical line keeps on moving towards the right also at larger volumes, presumably converging to a limit curve at infinite volume. Here we suppose that the real part of the zero lying next to the real axis is an estimation for the critical mass. The hypothesis that the imaginary part of the critical zero vanishes in the infinite volume limit has been explicitly checked by introducing a constant term in the scaling relation (11) and fitting the data to determine its value. In the interesting β region the value of the constant is compatible with zero.

The scaling analysis at this point is made using relations (10) and (11).

The strong dependence on the volume of the critical line implies that the scaling of the imaginary part of the critical zero should be checked at i) fixed β_c and ii) fixed critical mass. The latter case requires the knowledge of the critical zero at any β : this is done by interpolating the results obtained from a sufficiently dense set of β values. This is done here for a wide range of β_c and m_c .

In Fig.7 and Fig.8 we show the typical scaling behavior as a function of the volume for the imaginary part of the critical zero, at fixed $\beta_c = 0.885$ and fixed

$m_c = 0.05$ respectively. Similar results have been obtained at different β_c and m_c values.

From the slopes of the fitting lines we determine the scaling exponent $\frac{1}{\nu}$ as a function of β and m respectively. These are shown in Fig.9 and Fig.10. The results are compatible with the transition remaining first order down to $m = 0$.

In the large m region the situation is similar to the one observed at these volumes for the quenched theory [8]. We recall that in the quenched case the scaling exponents reach the first order value only for volumes larger than 10^4 . At the moment it is not clear why the introduction of dynamical fermions allows a faster convergence to the infinite volume regime.

We now turn to the scaling features on the real part of the critical zeros.

In Fig.11 we show the scaling behavior of the real part of the critical zero at $\beta_c = 0.885$; the infinite volume critical mass can be inferred using the Finite Size Scaling in Eq. 10. In principle this analysis, carried out for several values of β in the intermediate region, gives an estimation of the infinite volume critical mass as a function of the coupling constant. The corresponding analysis can be carried out also by fixing m_c and extracting the limiting value of the coupling constant. The critical points obtained with this method are reported in Fig.12. The superposition of the two sets gives us a clear signal of the reliability of our results.

We now discuss the scaling behavior of the linear density of the zeros lying next to the real axis. In Fig.13 we show these zeros at $\beta = 0.885$ for 6^4 , 8^4 and 10^4 lattices. The interesting feature of these patterns is that the zeros are exactly equispaced and the spacing is twice the distance of the critical zero from the real axis. Therefore the linear density has the same scaling properties as the imaginary part of the critical zero and this is exactly what one expects in the case of a first order phase transition. The situation holds also for different β . This property allows an unambiguous evaluation of the scaling exponent, independently from the different suitable definitions of the linear density.

6 Conclusions

We have presented in this paper an extensive analysis of the phase structure of the four-dimensional compact abelian model with fermionic degrees of freedom. This analysis has been made possible by the application of the powerful tool of the Lee-Yang zeros to the partition function obtained with two different methods, namely the Hybrid MonteCarlo method and the Microcanonical Fermionic Average method.

While the effectiveness and the problems of the HMC method are already well established, the application of the MFA method to the analysis of the critical properties of the L-Y zeros is new and powerful. In particular this approach makes possible to explore the coupling constants space at relatively small computer cost.

It is important to stress the fact that the two methods are completely independent, using totally different strategies and computational approaches. Given the structure of the fermionic determinant on the lattice, i.e. a huge polynomial with terms varying over an exponential range of order of magnitude, even tiny systematic effects are likely to manifest themselves in huge differences.

Still, the two methods give essentially equal results in the important critical regions. Systematic effects, where present, are well understood and completely under control.

From a technical point of view, it might be interesting to remark that the MFA approach allows a natural factorization of the generational and analysis steps: this is exemplified by the fact that of the simulations quoted in the paper, the 8^4 lattice uses the same configurations generated for the analysis reported in [9], only the analysis of the data being obviously different. Only those concerning the $4^4, 6^4, 10^4$ have been repeated or performed *ex novo*.

From a physical point of view, all the results we present are strongly supporting the picture of the phase transition of the theory being first order down to $m = 0$. In particular, we do not find any sign of softening of the transition due to the inclusion of fermionic degrees of freedom. Thus, the theory has no continuum limit. Even though these results have been obtained on small lattices, use of Finite Size Scaling analysis gives predictions of the infinite volume behaviour totally consistent with this picture. It has to be added that these results are consistent with the ones obtained in different approaches, so giving a consistent picture of the model.

We expect a totally different behaviour in the (possibly more interesting physically) case of the non compact model[7]. Here, the phase transition is entirely due to the presence of fermionic degrees of freedom; it is of second (or higher) order, so possibly defining a continuum theory. The important issue here is the (non) triviality of the theory at the critical point: a precise determination of the critical β is essential to assess the (non)triviality of the model. An analysis of the non compact QED (in dimensions ranging from 3 to 5) under the lines depicted above is underway and will be presented elsewhere.

7 Acknowledgements

V.A., R.B., G.D.C., A.F.G. and G.S. thank CICYT (Spain) - INFN (Italy) collaboration for partial support to this work.

References

- [1] C.N. Yang and T.D. Lee, Phys. Rev. **87**, 404 (1952).
T.D. Lee and C.N. Yang, Phys. Rev. **87**, 410 (1952).
- [2] M. Falcioni, E. Marinari, M.L. Paciello, G. Parisi and B. Taglienti, Phys. Lett. **B108**, 331 (1982);
G. Bhanot, S. Black, P. Carter and R. Salvador, Phys. Lett. **B183**, 331 (1987);
G. Bhanot, K. Bitar and R. Salvador, Phys. Lett. **B187**, 381 (1987); Phys. Lett. **B188**, 246 (1987).
- [3] R.B. Pearson, Phys. Rev. **B26**, 6285 (1982).
C. Itzykson, R.B. Pearson and J.B. Zuber, Nucl. Phys. **B220**, 415 (1988).
E. Marinari, Nucl. Phys. **B235**[FS11], 123 (1984).
- [4] M. Karliner, S.R. Sharpe and Y.F. Chang, Nucl.Phys. **B302**, 204 (1988) and references therein.
- [5] I.M. Barbour, A.J. Bell, M. Bernaschi, G. Salina, A. Vladikas, Nucl.Phys. **B386**, 683 (1992).
- [6] I.M. Barbour, A.J. Bell, E.G. Klepfish, Nucl.Phys. **B389**, 285 (1992).
- [7] A. Kocic, Nucl.Phys. **B34** (Proc. Suppl.), 129 (1994) and references therein.
- [8] V. Azcoiti, G. Di Carlo and A.F. Grillo, Phys. Lett. **B238**, 355 (1990); Phys. Lett. **B268**, 101 (1991).
L.A. Fernandez, A. Munoz Sudupe, R. Petronzio and A. Tarancon, Phys. Lett. **B267**, 100 (1991).
G. Bhanot, Th. Lippert, K. Shilling and P. Ueberholz, Nucl. Phys. **B378**, 633 (1992).
Recently, this scenario has been put under discussion. See for example:
C.B. Lang and T. Neuhaus, Nucl Phys **B 34** (Proc. Suppl.), 543 (1994) and reference therein.
See also: A. Bode, Th. Lippert and K. Shilling, Nucl Phys **B 34** (Proc. Suppl.), 549 (1994).
- [9] V. Azcoiti, G. Di Carlo, L.A. Fernandez, A. Galante, A.F. Grillo, V. Laliena, X.Q. Luo, C.E. Piedrafitra and A. Vladikas, Phys. Rev. **D48**, 402 (1993).
- [10] I.M. Barbour, A.J. Bell, E. G. Klepfish, R. Burioni, A. Vladikas and G. Salina, Nucl.Phys. **B30** (Proc. Suppl.), 339 (1993).
- [11] V. Azcoiti, G. Di Carlo and A.F. Grillo, Phys. Rev. Lett. **65**, 2239 (1990).
V. Azcoiti, A. Cruz, G. Di Carlo, A.F. Grillo and A. Vladikas, Phys. Rev. **D43**, 3487 (1991).
- [12] See for example: M.E. Fisher in *Lectures in Theoretical Physics*, Vol. VII C, The University of Colorado Press, Boulder (1965).
- [13] V. Azcoiti, A. Cruz, E. Dagotto, A. Moreo and A. Lugo, Phys. Lett. **B175**, 202 (1986).

- J.B. Kogut and E. Dagotto, Phys. Rev. Lett. **59**, 617 (1987).
E. Dagotto and J.B. Kogut, Nucl. Phys. **B295**, 123 (1988).
- [14] I.M. Barbour, R. Burioni and G. Salina, *The general distribution of Lee-Yang zeros in compact lattice QED*, Preprint Romel 93/969, Rome2 93/030.
- [15] S. Duane, A.D. Kennedy, B.J. Pendleton and D. Roweth, Phys. Lett. **B195**, 216 (1987).
R. Gupta, G.W. Kilcup and S.R. Sharpe Phys. Rev. **D38**, 1278 (1988).
- [16] C. Lanczos, J. Res. Nat. Bur. Standards **45**, 409 (1952).
I.M. Barbour, N. E. Behill, P. Gibbs, G. Schierholz and M. Teper, " The Lanczos Method in Lattice Gauge Theories " in: *The Recursion Method and its Applications*, Lecture notes in Physics, Springer, Berlin (1985).
- [17] S.L. Adler, Phys. Rev. **D23**, 2901 (1981).
M. Creutz, Phys. Rev. **D36**, 515 (1986).
- [18] I.M. Barbour, R. Burioni G. Di Carlo and G. Salina, Nucl.Phys. **B34** (Proc. Suppl.), 540 (1994).

Table 1: Parameters of the simulations for HMC method. Simulations have been performed on a CRAY YMP at the CINECA.

| L | β | m_0 | # Iterations for thermalisation | # Measurements |
|------|---------|-------|---------------------------------|----------------|
| 4 | 0.0 | 0.05 | 600 | 3200 |
| | 0.5 | 0.05 | 600 | 3200 |
| | 0.8 | 0.05 | 600 | 3200 |
| | 0.85 | 0.05 | 600 | 3200 |
| | 0.865 | 0.05 | 600 | 3200 |
| | 0.885 | 0.05 | 600 | 3200 |
| | | 0.16 | 400 | 300 |
| | | 0.28 | 400 | 300 |
| | 0.92 | 0.05 | 600 | 3200 |
| | 0.95 | 0.05 | 600 | 3200 |
| | 1.0 | 0.05 | 600 | 3200 |
| | 1.5 | 0.05 | 600 | 3200 |
| | 6 | 0.885 | 0.03 | 600 |
| 0.10 | | | 600 | 400 |
| 0.16 | | | 600 | 400 |
| 8 | 0.885 | 0.08 | 600 | 300 |

Table 2: Parameters of the simulations for MFA method. Simulations have been performed on the Transputer Networks of the Theory Group of the INFN Frascati National Laboratories.

| L | #Energies | # Configurations per Energy | # μ c Iterations between measurements |
|-------|-----------|-----------------------------|---|
| 4 | 32 | 1000 | 100 |
| 6(ap) | 12 | 300 | 200 |
| 6(p) | 12 | 300 | 200 |
| 8 | 12 | 100 | 600 |
| 10 | 12 | 30 | 1500 |

Table 3: Typical computer times required to generate the coefficients at different volumes for HMC and MFA.

| HMC | L | CRAY YMP hours (1β) | |
|-----|-----|-----------------------------|--|
| | 4 | 1.4 | |
| | 6 | 21.4 | |
| | 8 | 97.8 | |

| MFA | L | T800 hours (whole run) | CRAY YMP equiv. hours (whole run) |
|-----|-------|------------------------|-----------------------------------|
| | 4 | 500 | 2.2 |
| | 6(p) | 1440 | 6.4 |
| | 6(ap) | 1440 | 6.4 |
| | 8 | 4800 | 21.3 |
| | 10 | 8640 | 38.4 |

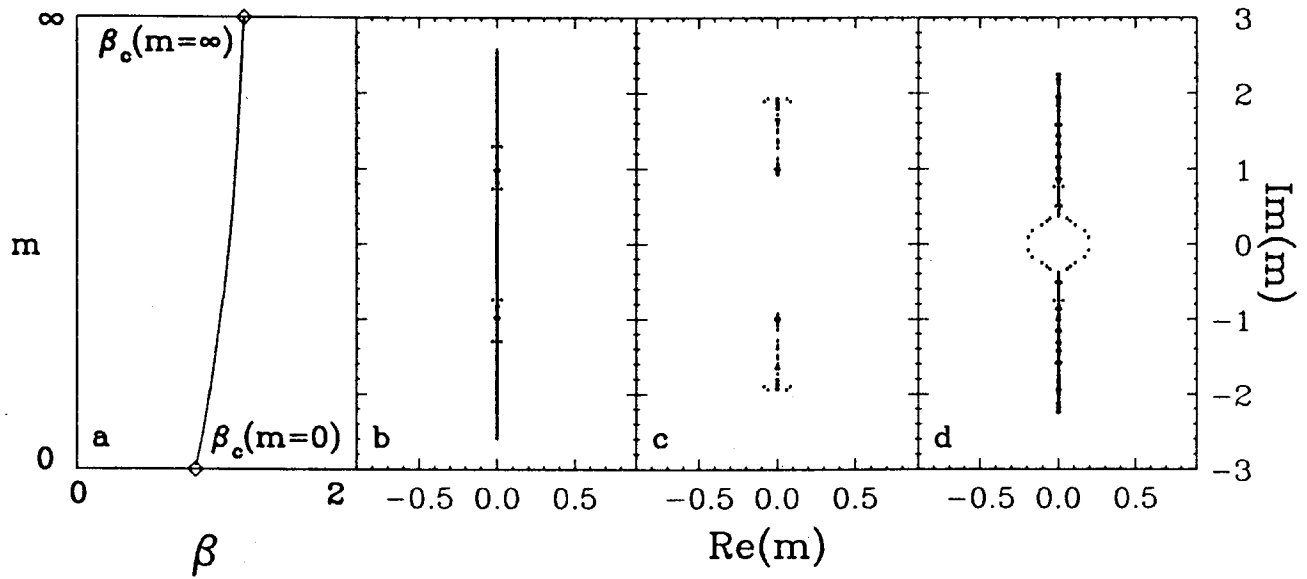


Fig. 1: Schematic phase diagram in the $m-\beta$ plane (a). Typical zero patterns at strong (b), weak (c) and intermediate coupling (d).

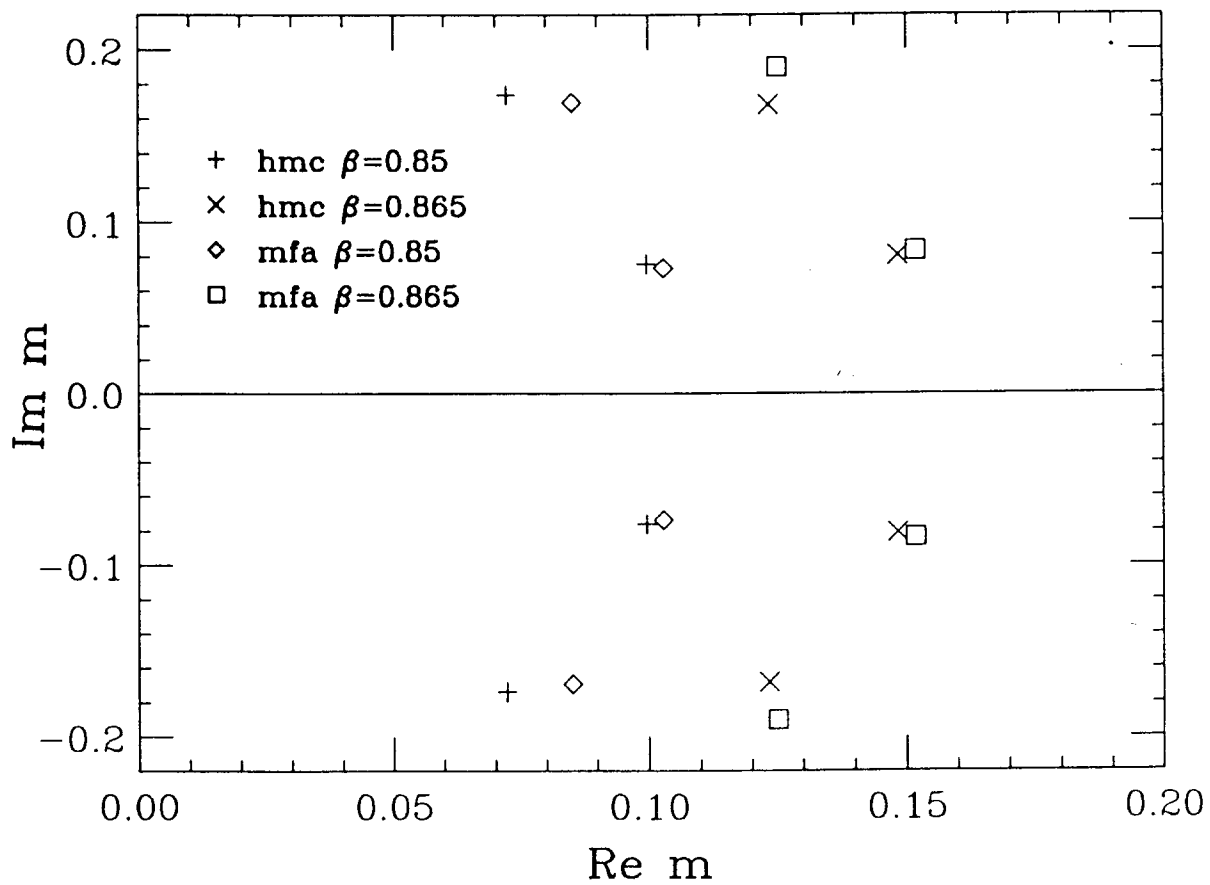


Fig. 2: Critical zeros on 4^4 lattice at $\beta = 0.85$ and $\beta = 0.865$ from HMC and MFA methods.

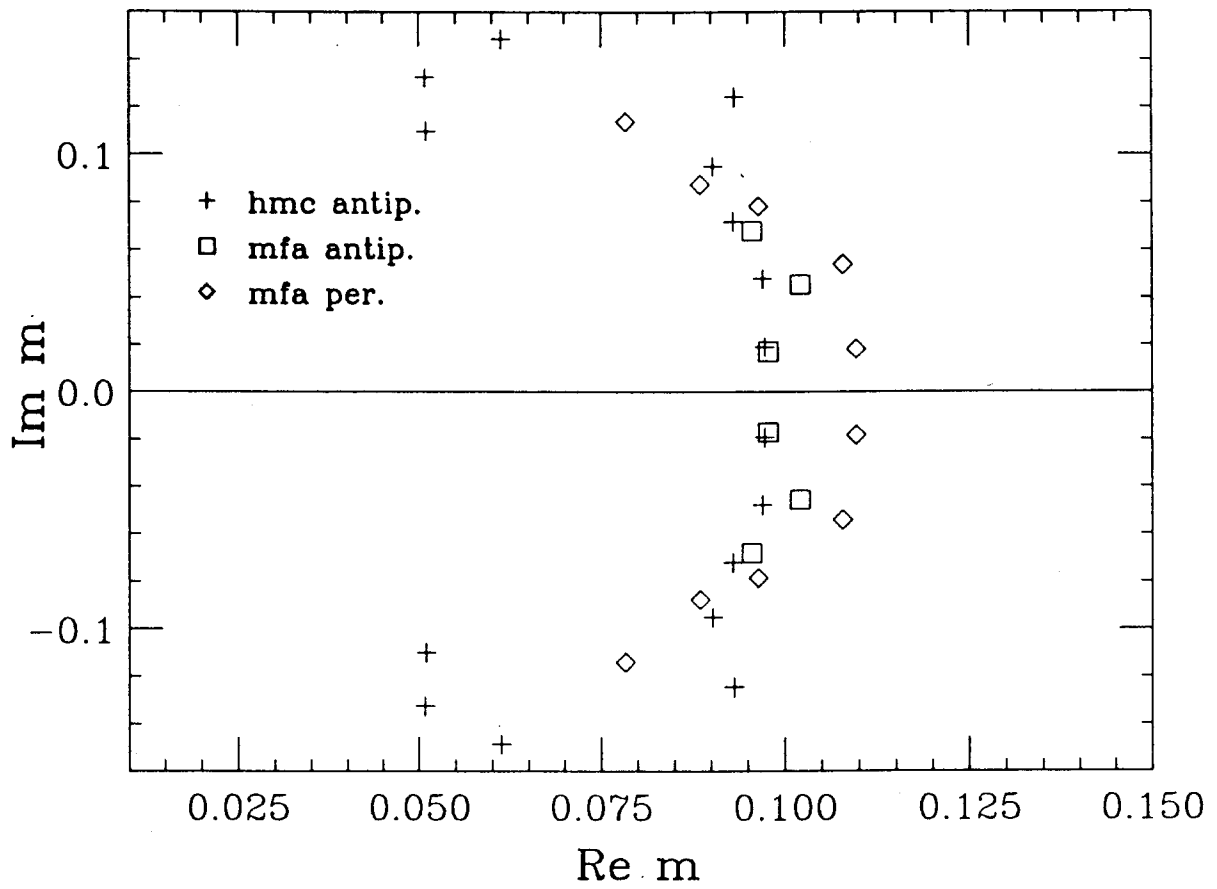


Fig. 3: Zero patterns on 6^4 lattice at $\beta = 0.885$ from HMC and MFA with periodic and antiperiodic boundary conditions. The errors ($\sim 10\%$) are not shown in the figure for simplicity sake.

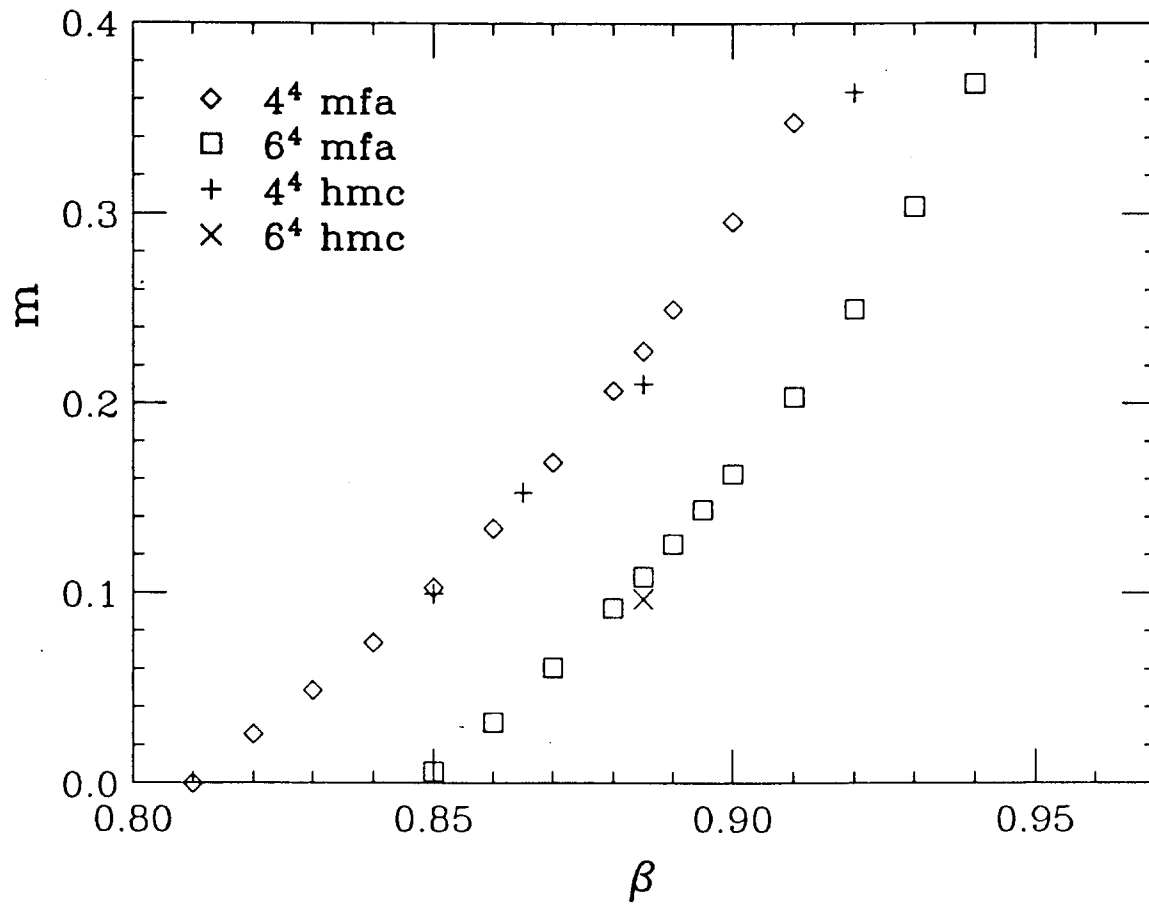


Fig. 4: Phase diagram in the $\beta - m$ plane on 4^4 and 6^4 lattices from MFA and HMC.

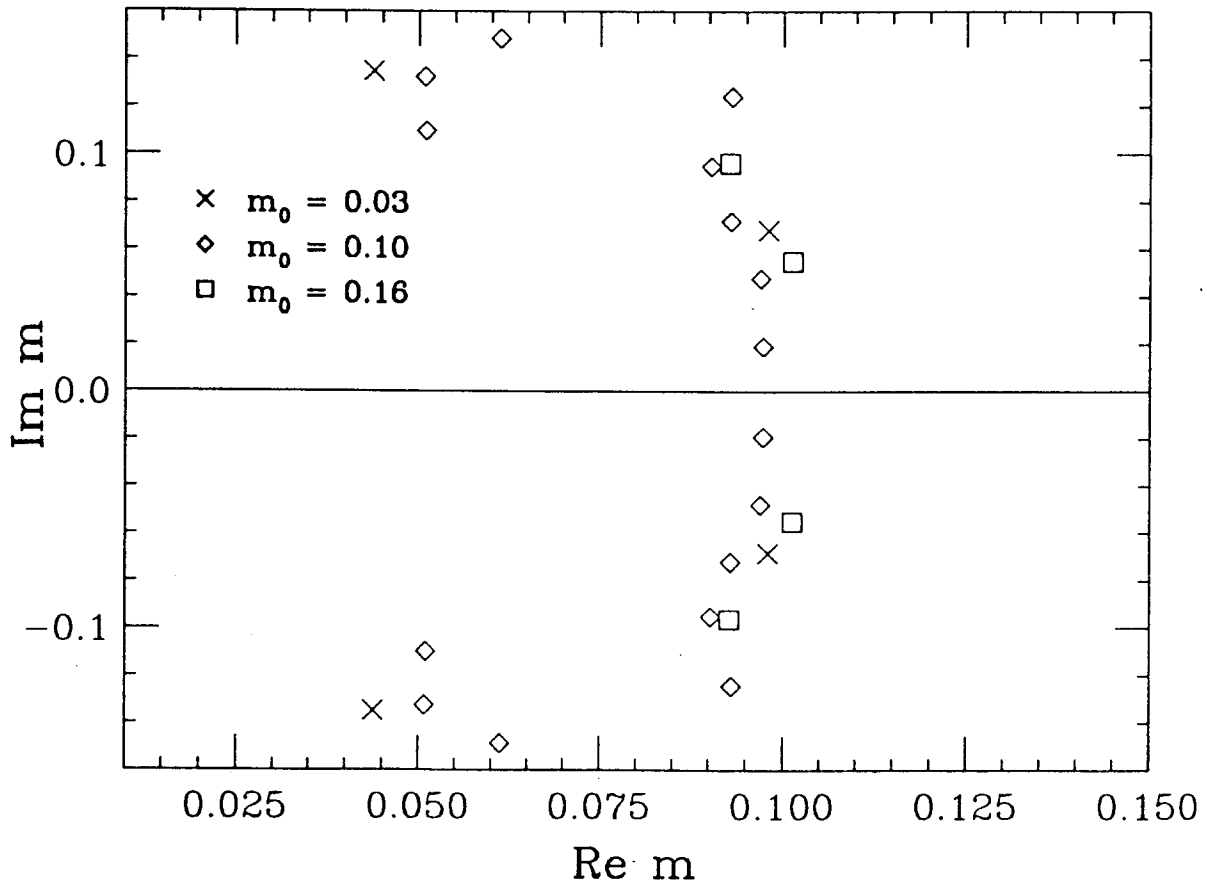


Fig. 5: Zero patterns on 6^4 lattice at $\beta = 0.885$ from HMC with three different values of m_0 .

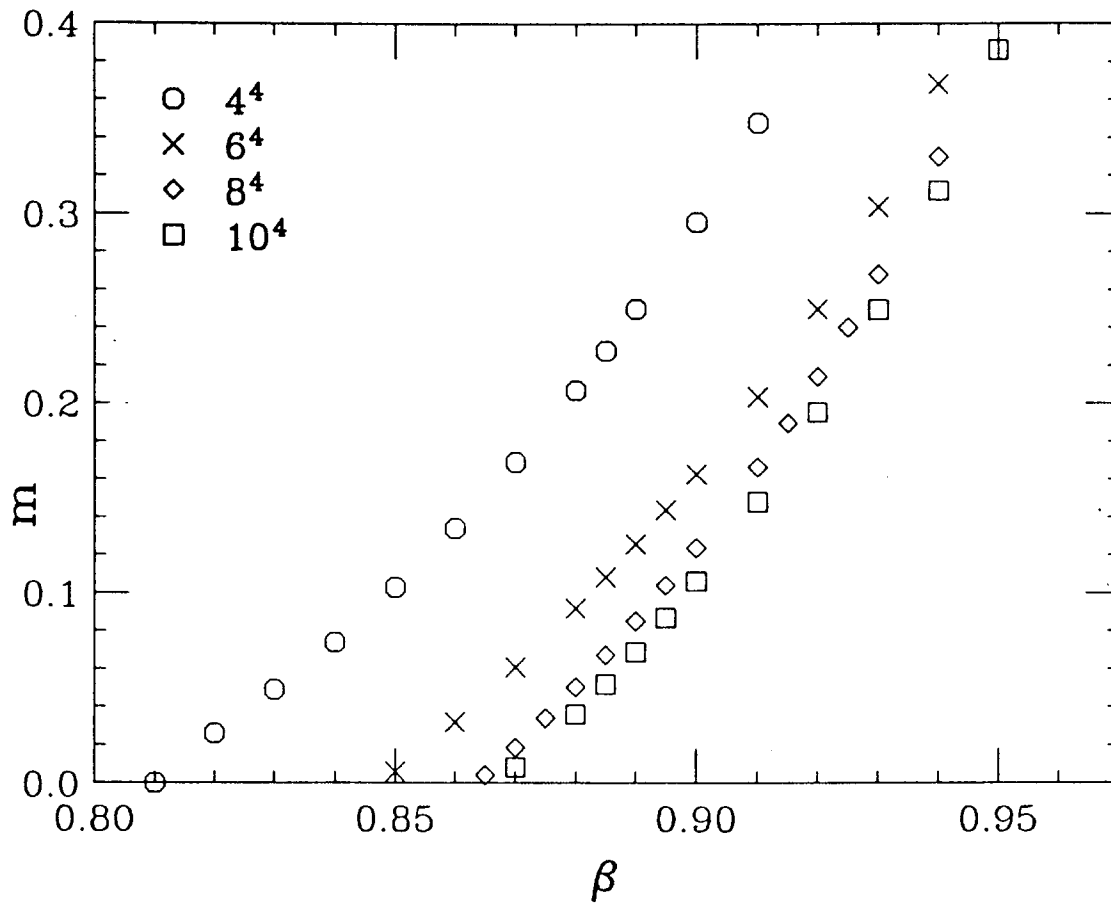


Fig. 6: Phase diagrams in the $\beta - m$ plane obtained on 4^4 , 6^4 , 8^4 and 10^4 lattices from MFA method.

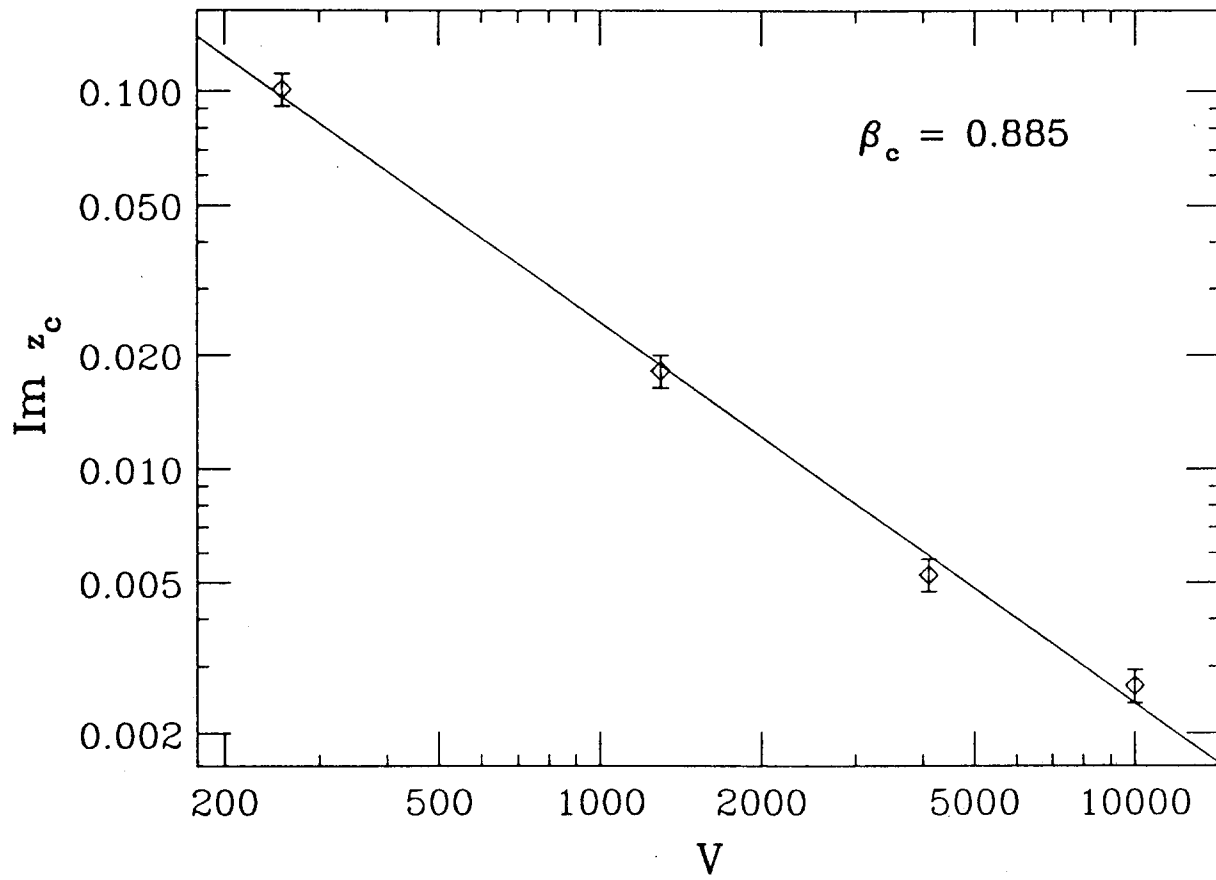


Fig. 7: Fit of the scaling behavior as a function of the volume for the imaginary part of the critical zero at fixed $\beta_c = 0.885$; $\chi^2 = 1.42$ per d.o.f..

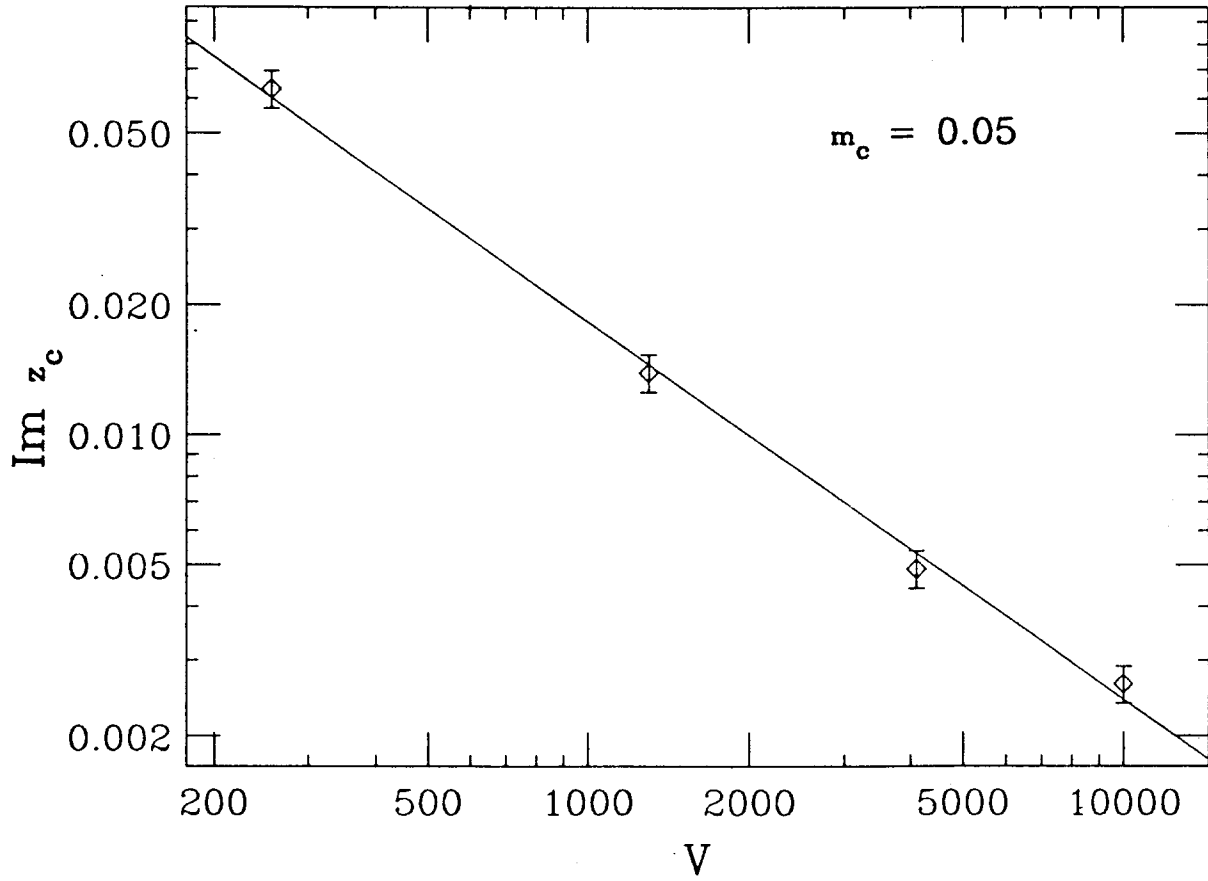


Fig. 8: Fit of the scaling behavior as a function of the volume for the imaginary part of the critical zero at fixed $m_c = 0.05$; $\chi^2 = 0.895$ per d.o.f..

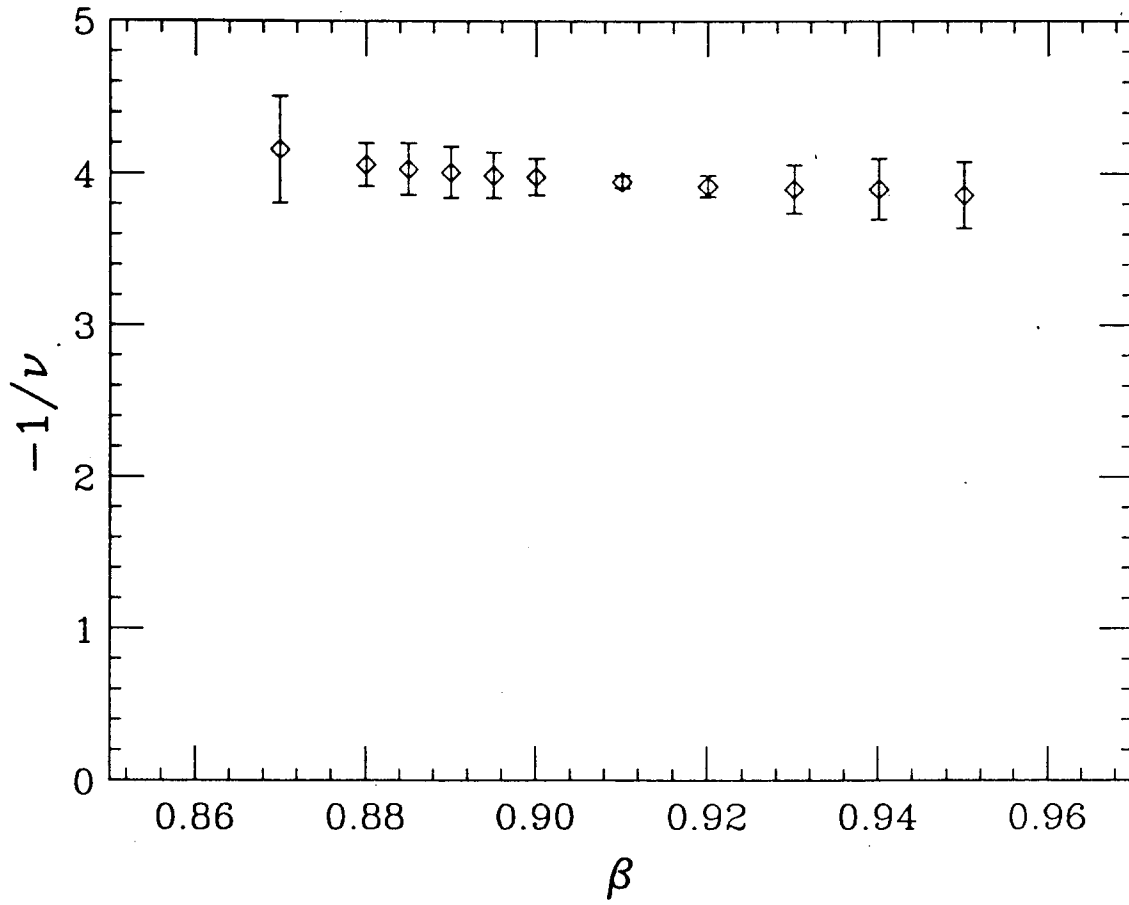


Fig. 9: Scaling exponent $\frac{1}{\nu}$ as a function of β .

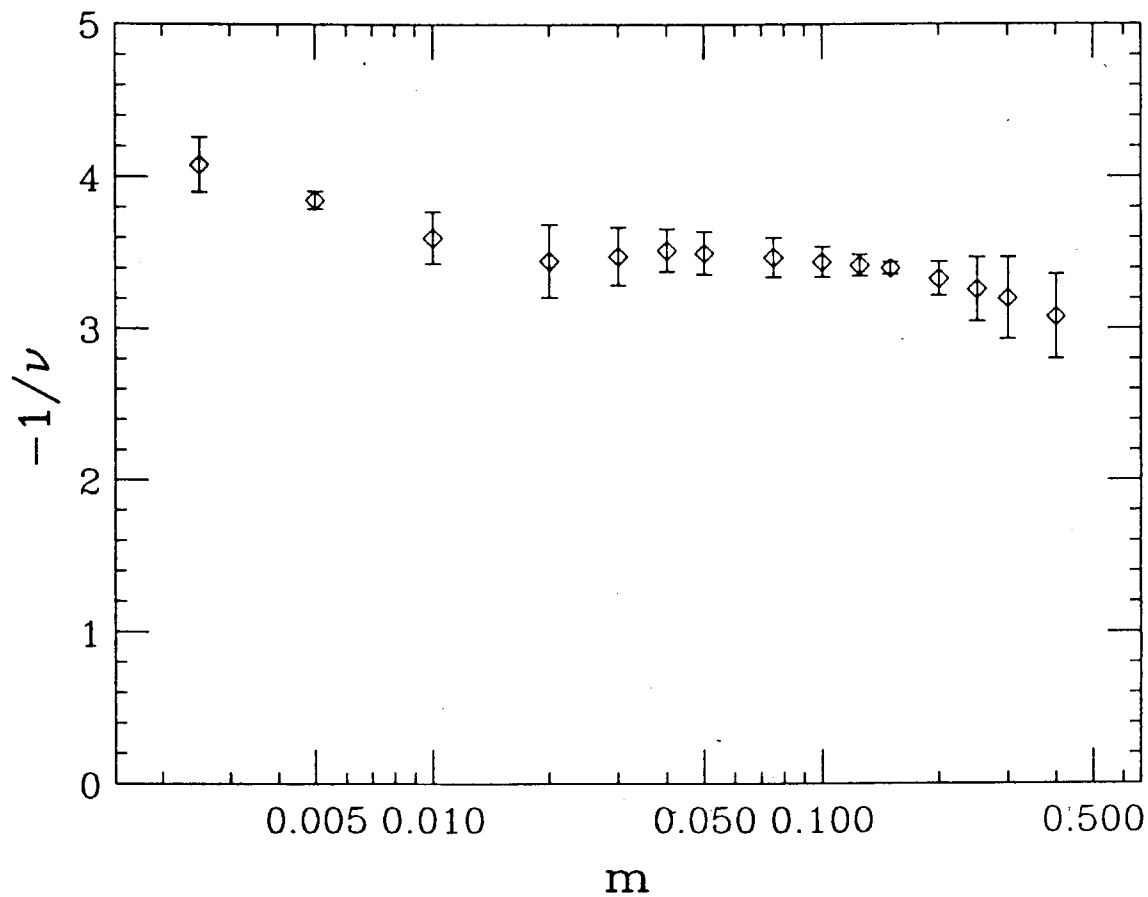


Fig. 10: Scaling exponent $\frac{1}{\nu}$ as a function of m (logarithmic scale).

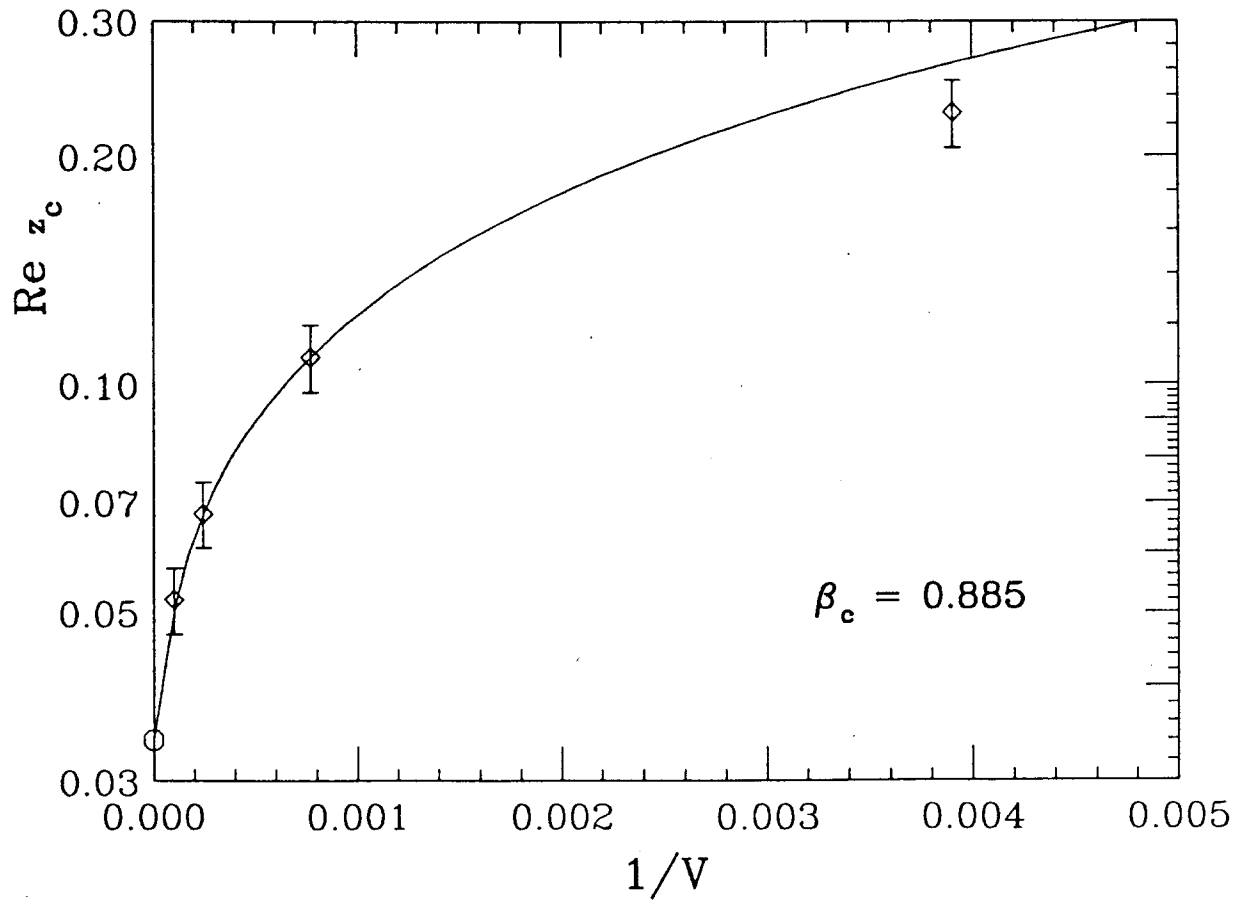


Fig. 11: Scaling behavior of the real part of the critical zero as a function of the inverse of the volume at $\beta_c = 0.885$. The circle is the estimate for the critical mass in the infinite volume limit obtained using 6^4 , 8^4 and 10^4 lattices.

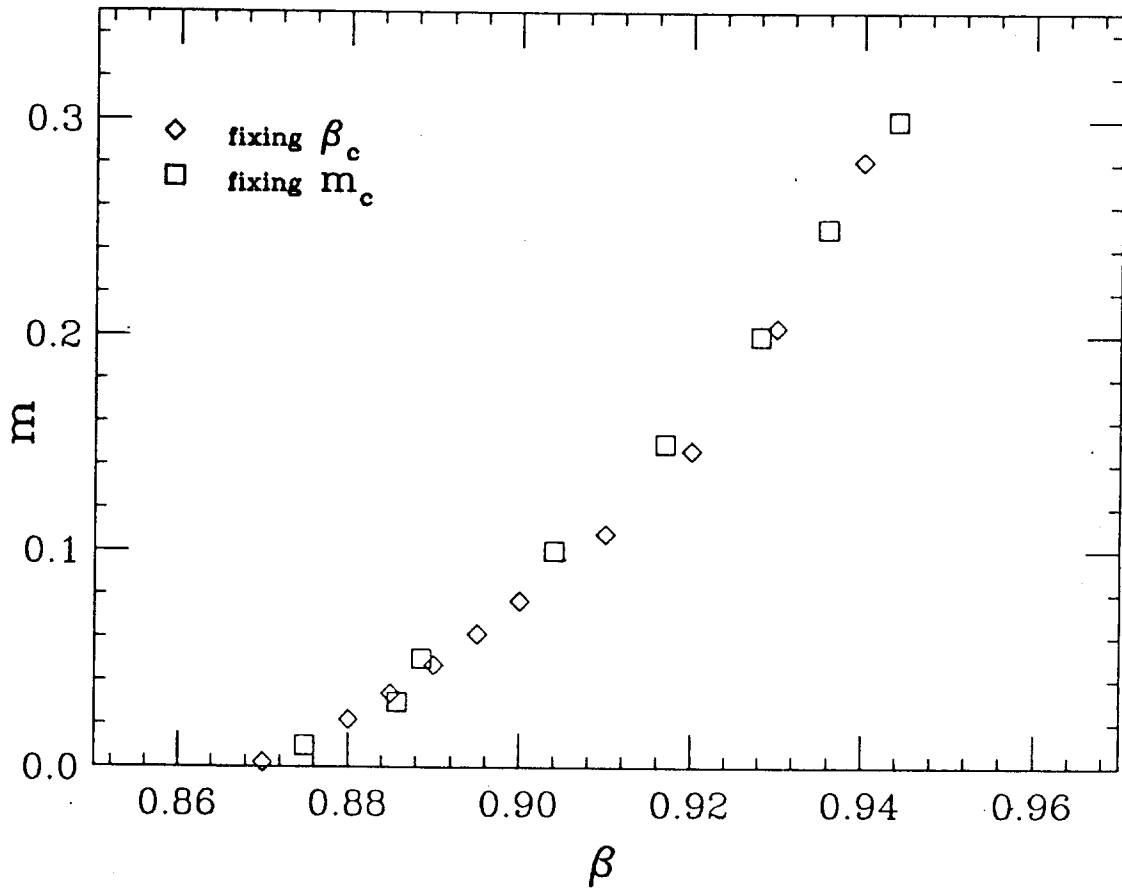


Fig. 12: Tentative phase diagram at infinite volume obtained from the scaling of the real part of the critical zero fixing β_c and m_c .

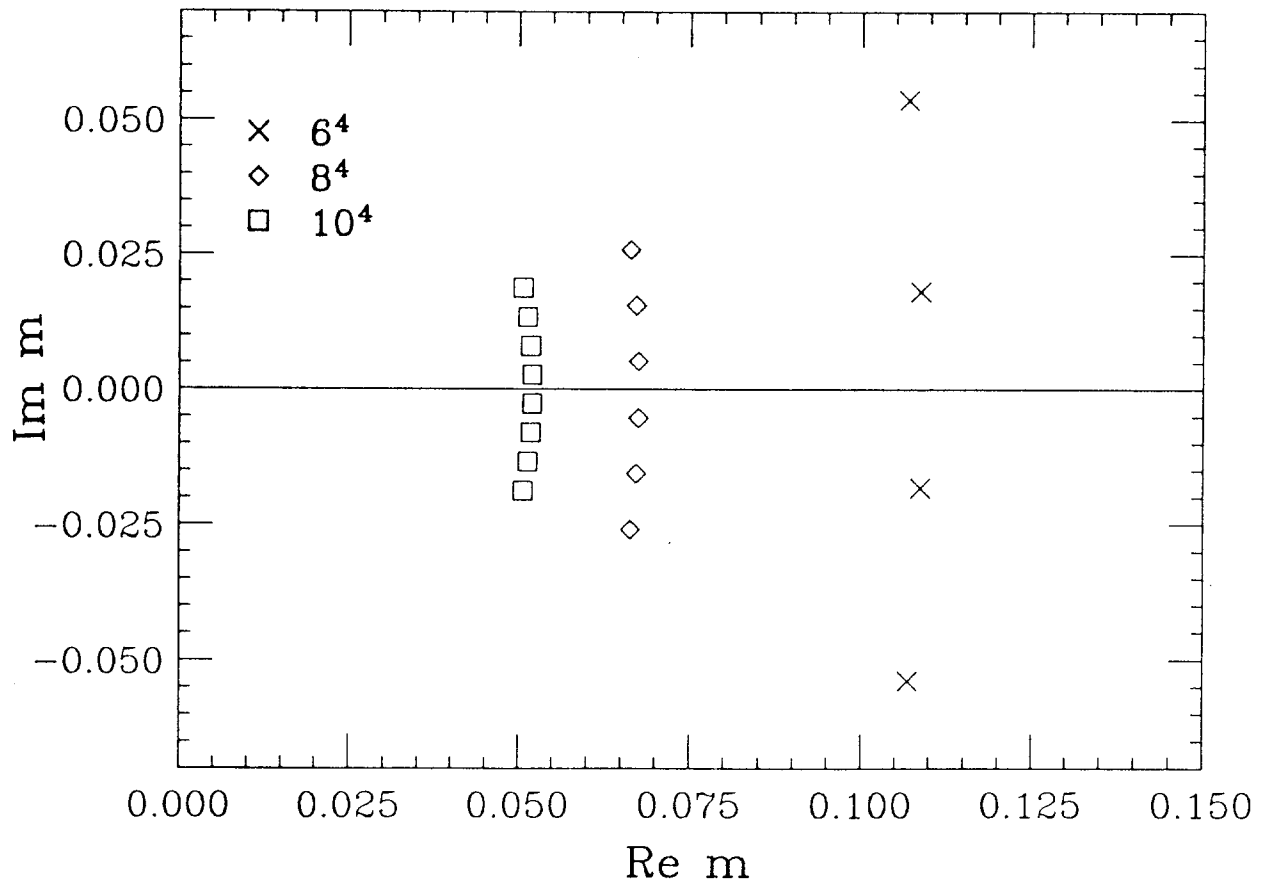


Fig. 13: Zero patterns at $\beta = 0.885$ for 6^4 , 8^4 and 10^4 lattices.

